Drug Design, Development and Therapy

Dovepress
Taylor & Francis Group

Open Access Full Text Article

ORIGINAL RESEARCH

Machine Learning Models Reveal New Risk Factors for Sub-/Supra-Therapeutic Concentrations of Sirolimus in Children with Vascular Anomalies

Ya-Hui Hu[1,*], Wan-Xia Li[2,3,*], Lin Fan[1,*], Zhou Zhou[3,*], Hong-Li Guo[1], Feng Chen[1], Jian-Jun Zou[3], Yi Ji[4], Jin Xu[1], Wei-Min Shen[4]

[1]Pharmaceutical Sciences Research Center, Department of Pharmacy, Children's Hospital of Nanjing Medical University, Nanjing, 210008, China; [2]School of Basic Medicine and Clinical Pharmacy, China Pharmaceutical University, Nanjing, 210009, China; [3]Department of Pharmacy, Nanjing First Hospital, Nanjing Medical University, Nanjing, 210006, China; [4]Department of Burns and Plastic Surgery, Children's Hospital of Nanjing Medical University, Nanjing, 210008, China

*These authors contributed equally to this work

Correspondence: Yi Ji; Wei-Min Shen, Children's Hospital of Nanjing Medical University, 72 Guangzhou Road, Nanjing, 210008, People's Republic of China, Email summer035@hotmail.com; swmswmswm@sina.com

Introduction: Sirolimus, also known as rapamycin, is an mTOR receptor inhibitor that suppresses cell proliferation and angiogenesis, demonstrating efficacy against multiple types of vascular anomalies. However, sub-therapeutic concentrations (below effective levels) and supra-therapeutic concentrations (leading to adverse reactions) of sirolimus may both negatively impact patient treatment outcomes. This study aimed to establish optimal models to predict the risk of sirolimus exposure using machine learning, ensure that sirolimus blood concentrations remain within the therapeutic range, and thus enhance the efficacy and safety of sirolimus therapy for children with vascular anomalies.

Methods: We retrospectively analyzed 134 sirolimus therapeutic drug monitoring (TDM) measurements from 49 patients. Data were randomly split into training (80%) and testing (20%) sets, with an additional temporal cohort for external validation. Six machine learning models were developed to predict sub-therapeutic and supra-therapeutic risks, and evaluated primarily by the area under the receiver operating characteristic curve (AUROC) and Brier score. The optimal model was interpreted using SHapley Additive exPlanations (SHAP) analysis.

Results: The sub-therapeutic risk model included body mass index (BMI), white blood cells (WBC), mean corpuscular hemoglobin (MCH), triglycerides (TG), and total bilirubin (TBIL); while the supra-therapeutic model comprised height, platelet count (PLT), alanine aminotransferase (ALT), high-density lipoprotein cholesterol (HDL), and total cholesterol (TC). The multilayer perceptron (MLP) and extreme gradient boosting (XGB) models showed optimal performance for sub-therapeutic (AUROC = 0.646, Brier = 0.190) and supra-therapeutic (AUROC = 0.825, Brier = 0.143) risk prediction, respectively, with consistent results in temporal validation (AUROC: 0.678, Brier = 0.190 and AUROC: 0.767, Brier = 0.190).

Conclusion: This study is the first to use machine learning models to predict the risk of sub- or supra-therapeutic sirolimus concentrations in vascular anomalies children. By enabling personalized exposure risk prediction, the dosing accuracy of sirolimus for the treatment of children with vascular anomalies can be optimized, thereby enhancing effectiveness and safety.

Keywords: sirolimus, vascular anomalies, machine learning, concentration risk prediction, children

Introduction

Sirolimus, also known as rapamycin, was initially discovered as an antifungal metabolite produced by *Streptomyces hygroscopicusis*.[1] It has now been approved by the US Food and Drug Administration (FDA) for the prevention of organ

https://doi.org/10.2147/DDDT.S563637
Received: 27 August 2025
Accepted: 12 December 2025
Published: 8 January 2026

transplant rejection and anti-seizure therapy in Tuberous Sclerosis Complex.[2] Over the past few decades, sirolimus has been used as an immunosuppressive, antiangiogenic, and cytostatic agent in clinical practice, and exhibits a beneficial role in the management of vascular anomalies.[3,4] Vascular anomalies represent a group of highly heterogeneous disorders, encompassing vascular tumors, vascular malformations, and potentially unique vascular anomaly,[5] which differ significantly in their natural history and management objectives. Clinically, sirolimus was first tested on an off-label basis in patients with complex life-threatening vascular anomalies.[6] Multiple retrospective analyses and prospective clinical trials have since confirmed the efficacy and tolerability of sirolimus. Approximately 50% to 90% of patients experienced symptomatic improvement, such as reduced pain, improved function, stopped the oozing and infectious episodes within 3 months.[7–11] The most frequent adverse events of oral sirolimus in vascular anomalies include asthenia, mucositis, acneiform eruptionle, headache, hypercholesterolemia, diarrhea, and nausea.[12–14]

Sirolimus is primarily metabolized by cytochrome P450 3A4/5 and CYP2C8 enzymes. It is also a substrate of the P-glycoprotein (P-gp, encoded by the *ABCB1* gene) efflux pump.[15] Multiple factors influence drug exposure, including age, ethnicity, disease status, dietary habits, drug–drug interactions, and polymorphisms in *CYP3A4/5* and *ABCB1* genes.[16–20] Patients exhibit very large interindividual variability (44% to 52%) and intraindividual variability (14% to 88%) in the pharmacokinetics of sirolimus.[21–23] Sirolimus is an important therapeutic option for vascular anomalies, and therefore, adequate monitoring is necessary. Therapeutic drug monitoring (TDM) provides a strategy for tailoring individualized medication regimens to avoid exposure-related drug toxicity as well as reduce treatment failure rates.[24] Early systematic reviews indicated that the most commonly recommended sirolimus trough concentration target ranges in pediatric populations with vascular anomalies are 5 to 15 ng/mL or 10 to 15 ng/mL.[25,26] Current guidelines for sirolimus in vascular anomalies emphasize that monthly blood concentration monitoring should be performed for specific disease subtypes, for instance, kaposiform hemangioendothelioma (KHE), tufted angioma (TA), and lymphatic malformation (LM), with trough levels maintained between 10 and 15 ng/mL.[27,28] Although existing population pharmacokinetic (PPK) models aid in initial sirolimus dosing, maintaining drug concentrations at target exposures throughout the treatment period remains challenging.[29–32] Our previous research has revealed that even with regular and timely monitoring of the blood concentration of sirolimus, only 54% of the patients could maintain concentrations with the target range (10–15 ng/mL).[33] Therefore, it is imperative to adopt innovative strategies to improve the precision of dosing.

Machine learning (ML) is a data-driven methodology that employs various algorithms to learn from training data, thereby enabling prediction and decision-making for specific events.[34] In the field of individualized precision treatment, there is a growing interest in the application of ML algorithms for data analysis and predictive modeling to guide more accurate diagnoses, personalized treatment strategies, and prognostic prediction.[35–37] In the management of vascular anomalies, ML-based radiomic models have been widely applied to medical imaging analysis, especially in diagnosis, assessment of treatment response, prediction of outcomes and prognosis based on a combination of imaging and pathology data.[38–40] Beyond imaging, ML excels at identifying complex, nonlinear patterns and interactions within multifactorial data without requiring a predefined structural model. It can therefore go beyond the constraints of traditional parametric models[20] to suggest previously unrecognized predictors of interindividual pharmacokinetic variation. By learning directly from historical TDM data and accompanying patient characteristics, ML models can generate personalized risk predictions.[41,42] This capability enables more proactive and preemptive dose adjustment strategies, with the potential to surpass the reactive nature of traditional TDM. As such, ML represents a promising emerging approach to guide TDM and personalized dosing, and ML algorithms are promising for predicting sirolimus exposure in vascular anomalies populations.

This study aims to identify significant risk factors influencing sirolimus concentrations and to develop ML models for predicting the risk of sub-/supra-therapeutic sirolimus levels, facilitating the maintenance of therapeutic drug levels within the 10–15 ng/mL range to optimize therapeutic efficacy while minimizing toxicity risks in vascular anomalies children.

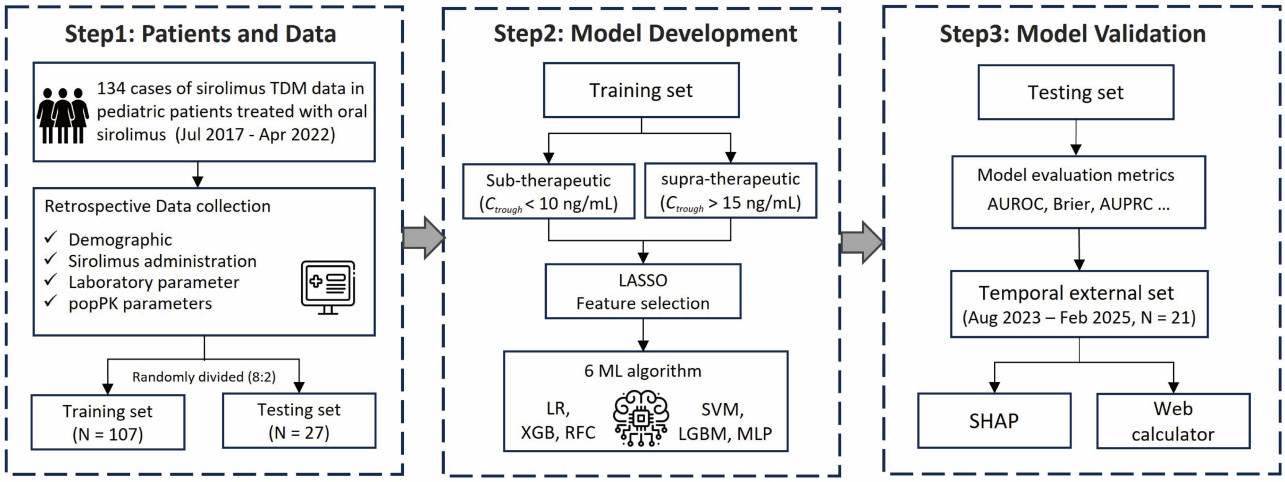

Figure 1 Workflow of the study design.
Abbreviations: TDM, therapeutic drug monitoring; LASSO, least absolute shrinkage and selection operator; AUROC, area under the receiver operating characteristic curve; AUPRC, area under the precision–recall curve; SHAP, SHapley Additive exPlanations.

Methods

Study Population

This retrospective study analyzed pediatric patients receiving oral sirolimus therapy at Children's Hospital of Nanjing Medical University between July 2017 and April 2022, with inclusion criteria comprising: (1) diagnosis of vascular anomalies and (2) undergoing sirolimus TDM, while exclusion criteria included: (1) values exceed the limits for detection, (2) ongoing severe infections, and (3) multiorgan dysfunction. The study protocol received approval from the Ethics Committee of the Children's Hospital of Nanjing Medical University (Approval No.202206114–1). The overall study scheme is presented in Figure 1.

Sample Analyzing

The initial dosage of sirolimus was 0.1 mg/kg/day or 0.8 mg/m^2/day, with subsequent adjustment based on the sirolimus blood concentration target of 10–15 ng/mL. Whole blood samples are routinely transported to the laboratory for blood concentration monitoring during sirolimus treatment. The bioanalytical performance can be found in our previously published study.[43] Briefly, approximately 1 mL of peripheral blood was collected into an ethylenediaminetetraacetic acid (EDTA)-K2 anticoagulant tube for TDM 30 minutes prior to the next scheduled sirolimus administration. A 200 μL aliquot of whole blood was mixed with 200 μL methanol and 50 μL of the sample pretreatment reagent (Siemens Healthcare Diagnostics Inc.), vortexed thoroughly, and centrifuged at 12,000 rpm for 5 minutes at 4°C. The resulting supernatant was analyzed using an automated enzyme immunoassay analyzer (SIEMENS, Munich, Germany). The analytical performance was validated through the External Quality Assessment Scheme administered by the National Center for Clinical Laboratories.

Data Collection and Processing

Patient data were extracted retrospectively from the electronic hospital information system. The data encompassed the following aspects: (1) Demographic information, including age, sex, etc.; (2) Sirolimus administration details, such as dose and interval; and (3) Laboratory parameters, including white blood cell count (WBC), platelet count (PLT), etc. Additionally, (4) the apparent clearance (CL/F) and apparent distribution volume (V/F) for each patient were calculated using a previously constructed population pharmacokinetic (PPK) model.[30] The specific formula is as follows:

$$CL/F = 4.06 \times \left(\frac{\mathrm{BW}}{16}\right)^{1.23};\ V/F = 155 \times \left(\frac{\mathrm{BW}}{16}\right)^{1.62}$$

https://doi.org/10.2147/DDDT.S563637

A total of 28 features were initially included as potential predictors for subsequent feature selection. As the period between two TDM tests for the same patient was principally in excess of one month, the samples could be considered mutually independent.[44] Moreover, we transformed sirolimus blood concentration into a categorical variable based on its target therapeutic ranges.[45] Specifically, a value of 1 was assigned for sub-therapeutic outcome when the concentration was < 10 ng/mL, and 0 otherwise; for the supra-therapeutic outcome, a value of 1 was assigned when the concentration was > 15 ng/mL, and 0 otherwise.

The dataset was randomly divided into two sets: an 80% training set for feature selection and model development, and a 20% testing set for model evaluation. Missing data were imputed separately in each set: continuous variables were handled using k-nearest neighbors (KNN) imputation, while categorical variables were imputed using the mode. Prior to modeling, continuous and multi-class categorical variables were standardized using Z-score normalization and one-hot encoding, respectively.

Modelling and Validation

For both sub-therapeutic and supra-therapeutic outcomes, feature selection was performed uniformly using least absolute shrinkage and selection operator (LASSO) regression. The LASSO algorithm eliminates weakly associated features by shrinking their coefficients to zero via λ optimization while retaining the most predictive feature subset.[46] Furthermore, multicollinearity among selected variables was assessed using variance inflation factors (VIF), with VIF < 5 was considered insignificant.

We systematically evaluated six ML algorithms, including logistic regression (LR), extreme gradient boosting (XGB), random forest classifier (RFC), support vector machine (SVM), light gradient boosting machine (LGBM), and multilayer perceptron (MLP), with all model hyperparameters optimized through a 5-fold cross-validated grid search algorithm, using a random state of 1 for both model initialization and the cross-validation process. The models were developed using Python 3.12.3 with "sklearn 1.6.1", "xgboost 2.1.4", and "lightgbm 4.6.0" packages.

The final models for both outcomes were selected based on a unified, objective criterion: the area under the receiver operating characteristic curve (AUROC) as the primary metric for discrimination, supplemented by the Brier score and calibration curves for calibration evaluation. The optimal classification threshold for each model was determined by maximizing Youden's index (J = sensitivity + specificity − 1).[47] Additional metrics including area under the precision–recall curve (AUPRC), precision, accuracy, recall, and F1-score were calculated for comprehensive performance assessment. The best-performing model was selected for further external validation, visualization, and deployment based on this multi-metric evaluation.

Temporal External Validation of the Best Model

An independent cohort collected from the same medical center between August 2023 and February 2025 was used for temporal validation of the final selected models for sub-therapeutic and supra-therapeutic risk prediction. The AUROC and Brier score were used to assess the performance of the prediction model.

Model Interpretation and Application

In order to enhance the interpretability of the model, SHapley Additive exPlanations (SHAP) analysis was employed to quantify feature contributions in the optimal models. Global model interpretation was performed using SHAP feature importance bar plots (ranking predictor contributions) and beeswarm plots (visualizing directional relationships), which collectively elucidate both the relative importance of features and their positive or negative associations with the outcome. The finalized models were subsequently deployed as a web-based tool for clinical use.

Statistical Analysis

Normality was assessed using the Shapiro–Wilk test. Variables described as mean ± standard deviation (SD) were analyzed using a *t*-test, while those described as median (interquartile range [IQR]) were compared using Mann–Whitney *U*-tests. Categorical variables were analyzed with the χ^2-test or Fisher's exact test, depending on the data distribution and sample size. A two-tailed p-value <0.05 was considered statistically significant. All analyses were conducted using R version 4.2.2 with the "Tableone" package.

Table 1 Baseline Characteristics of the Overall Cohort and Stratified by Training and Testing Sets

Characteristics	Overall (n = 134)	Training Set (n = 107)	Testing Set (n = 27)	P
Predict outcome				
Sirolimus concentration, ng/mL	12.25 [9.60, 15.17]	12.40 [9.55, 15.30]	11.80 [10.00, 14.30]	0.585
Therapeutic ranges, n (%)				0.601
Sub-therapeutic (<10 ng/mL)	40 (29.9)	33 (30.8)	7 (25.9)	
Therapeutic (10–15 ng/mL)	58 (43.3)	44 (41.1)	14 (51.9)	
Supra-therapeutic (>15 ng/mL)	36 (26.9)	30 (28.0)	6 (22.2)	
Demographic				
Age, y	3.50 [1.44, 6.04]	3.50 [1.46, 6.08]	3.33 [1.67, 5.46]	0.822
Sex, male/female	67/67	54/53	13/14	1.000
Height, cm	100.30 (25.92)	100.17 (23.89)	100.81 (33.34)	0.908
BW, kg	16.00 [12.00, 21.50]	16.50 [11.75, 21.50]	15.00 [12.25, 22.25]	0.816
BMI, kg/m^2	16.64 [15.39, 18.14]	16.41 [15.40, 18.11]	17.12 [15.00, 18.27]	0.573
Sirolimus administration				
Dose, mg	0.80 [0.50, 1.00]	0.80 [0.50, 1.00]	0.75 [0.50, 1.00]	0.737
Interval, h	12.00 [12.00, 12.00]	12.00 [12.00, 12.00]	12.00 [12.00, 12.00]	0.184
Laboratory parameter				
RBC, $10^{12}/L$	4.61 [4.28, 4.80]	4.63 [4.34, 4.80]	4.61 [4.03, 4.78]	0.183
WBC, $10^9/L$	8.00 [6.71, 9.45]	8.17 [7.10, 9.57]	7.48 [6.17, 8.89]	0.110
PLT, $10^9/L$	290.00 [253.25, 348.00]	289.00 [254.50, 347.50]	298.13 [247.00, 376.50]	0.647
HGB, g/L	120.56 [115.00, 126.75]	121.00 [116.00, 126.50]	118.00 [106.00, 126.00]	0.140
MCH, pg	26.70 [25.45, 27.67]	26.60 [25.50, 27.50]	26.80 [25.45, 28.55]	0.594
MCHC, g/L	330.00 [324.00, 338.00]	330.00 [324.00, 338.00]	330.00 [321.50, 337.00]	0.976
HCT, %	36.60 [34.73, 38.18]	36.80 [35.15, 38.05]	35.70 [33.00, 38.55]	0.205
ALB, g/L	44.73 (2.91)	45.08 (2.60)	43.34 (3.64)	0.005
ALT, U/L	12.00 [9.00, 15.10]	12.00 [9.00, 15.00]	13.00 [9.62, 17.00]	0.381
AST, U/L	26.50 [23.00, 32.00]	27.00 [23.00, 32.00]	26.00 [23.00, 32.00]	0.962
HDL, mmol/L	1.32 (0.36)	1.35 (0.36)	1.23 (0.37)	0.140
TG, mmol/L	1.03 [0.74, 1.27]	1.03 [0.74, 1.24]	1.04 [0.76, 1.43]	0.651
TC, mmol/L	4.15 [3.73, 4.58]	4.15 [3.74, 4.59]	4.15 [3.64, 4.31]	0.520
TBIL, μmol/L	5.20 [3.70, 7.16]	5.21 [3.70, 7.28]	5.10 [3.35, 6.58]	0.490
DBIL, μmol/L	1.97 [1.50, 2.59]	1.97 [1.50, 2.60]	2.11 [1.55, 2.30]	0.938
SCR, μmol/L	27.45 [23.50, 34.00]	27.40 [23.23, 33.00]	27.50 [25.00, 35.20]	0.564
BUN, mmol/L	4.30 (1.25)	4.37 (1.27)	4.04 (1.17)	0.225
UA, μmol/L	225.07 (55.80)	224.72 (53.33)	226.46 (65.81)	0.885
CYS, mg/L	0.97 [0.85, 1.14]	0.97 [0.85, 1.15]	0.94 [0.86, 1.09]	0.934
PPK parameters				
CL/F, L/h	4.06 [2.85, 5.84]	4.22 [2.78, 5.84]	3.75 [2.92, 6.09]	0.816
V/F, L	155.00 [97.26, 250.15]	162.92 [94.02, 250.15]	139.61 [100.59, 264.59]	0.816

Abbreviations: BW, body weight; BMI, body mass index; RBC, red blood cell count; WBC, white blood cell count; PLT, platelet count; HGB, hemoglobin; MCH, mean corpuscular hemoglobin; MCHC, mean corpuscular hemoglobin concentration; HCT, hematocrit; ALB, albumin; ALT, alanine aminotransferase; AST, aspartate amino transferase; HDL, high-density lipoprotein cholesterol; TG, triglycerides; TC, total cholesterol; TBIL, total bilirubin; DBIL, direct bilirubin; SCR, serum creatinine; BUN, blood urea nitrogen; UA, uric acid; CYS; cystatin C; PPK, population pharmacokinetic; CL/F, apparent clearance; V/F, apparent distribution volume.

Results

Baseline Patient Characteristics

This study comprised 134 TDM data cases of sirolimus treatment from 49 patients, with 107 assigned to the training set and 27 to the testing set. The whole cohort had a median age of 3.5 years (IQR 1.44–6.04) and median weight of 16 kg (IQR 12–21.5). Sirolimus blood concentrations were categorized into three therapeutic ranges: sub-therapeutic (n = 40, 29.9%), therapeutic (n = 58, 43.3%), and supra-therapeutic (n = 36, 26.9%). Baseline characteristics were well balanced between training and testing sets, as confirmed by inter-group comparisons (Table 1).

https://doi.org/10.2147/DDDT.S563637

Table 2 LASSO Selection Variables and Collinearity Analysis in Two Models

Sub-therapeutic Model			Supra-therapeutic Model		
Variables	**Coefficient**	**VIF**	**Variables**	**Coefficient**	**VIF**
BMI	0.000021	1.059563	Height	−0.002749	1.304037
WBC	0.042563	1.017267	PLT	0.000374	1.051299
MCH	−0.013085	1.008587	ALT	0.000984	1.274341
TG	0.121933	1.173216	HDL	−0.346883	1.745698
TBIL	−0.005400	1.206307	TC	0.292060	1.793492

Abbreviations: LASSO, least absolute shrinkage and selection operator; VIF, least absolute shrinkage and selection operator; BMI, body mass index; WBC, white blood cell count; MCH, mean corpuscular hemoglobin; TG, triglycerides; TBIL, total bilirubin; PLT, platelet count; ALT, alanine aminotransferase; HDL, high-density lipoprotein cholesterol; TC, total cholesterol.

Feature Selection and Correlation Analysis

Distinct feature sets were selected by LASSO regression for sub-therapeutic and supra-therapeutic outcomes. For sub-therapeutic risk prediction, the model retained body mass index (BMI), WBC, mean corpuscular hemoglobin (MCH), triglycerides (TG) and total bilirubin (TBIL). In contrast, the supra-therapeutic risk model incorporated height, PLT, high-density lipoprotein cholesterol (HDL), alanine aminotransferase (ALT), and total cholesterol (TC). The LASSO coefficients of specific features and their variance inflation factor (VIF) scores for multicollinearity assessment are shown in Table 2.

Additionally, we selected specific features that were potentially associated with patients' pharmacokinetic parameters, namely BMI, height, and body weight (BW). Subsequently, a matrix scatterplot analysis was conducted in order to comprehensively assess the potential relationships between these selected features and CL/F, V/F. As illustrated in Figure 2, BMI exhibited a relatively weak correlation with CL/F and V/F (Spearman's r = −0.200), while strong correlations were observed among the other features.

Model Performance

Six ML models were constructed using the two distinct feature sets described above. The optimal hyperparameters of each model are detailed in Supplementary Table S1. Performance metrics on the training set are presented in Supplementary Table S2 and Supplementary Figure S1, while the results of testing set are shown in Table 3 and Figure 3. Based on the discriminative ability and calibration in the testing set, the following models were selected: (1) Sub-therapeutic risk prediction: MLP (AUROC = 0.646, Brier = 0.190); (2) Supra-therapeutic risk: XGB (AUROC = 0.825, Brier = 0.143).

Temporal External Validation

The temporal validation cohort consisted of 21 cases of sirolimus TDM data, including 6 cases (28.6%) each of sub-therapeutic and supra-therapeutic outcomes. As demonstrated in Figure 4, the sub-therapeutic risk prediction model achieved an AUROC of 0.678 with a Brier score of 0.190. For supra-therapeutic risk prediction, the model demonstrated better discriminative ability with an AUROC of 0.767 and a Brier score of 0.178.

Model Interpretation and Deployment

The SHAP algorithm was employed to interpret feature importance and predictive contributions in our models. As illustrated in Figure 5, features were ranked by descending mean absolute SHAP values, where point coloration represents prediction magnitudes and rightward-distributed red points indicate positive correlations with outcome risk. In the sub-therapeutic risk model, MCH exhibited the highest feature importance. Notably, MCH and TBIL served as protective factors, whereas other variables were identified as risk factors. For the supra-therapeutic risk model, TC, height, HDL, and PLT had similar contribution magnitudes, with height and HDL acted as protective factors.

To facilitate clinical translation, we deployed the developed sub-therapeutic and supra-therapeutic risk prediction models as cloud-based web applications (available at: https://sirolimus-sub-therapeutic-risk-model.streamlit.app/ and

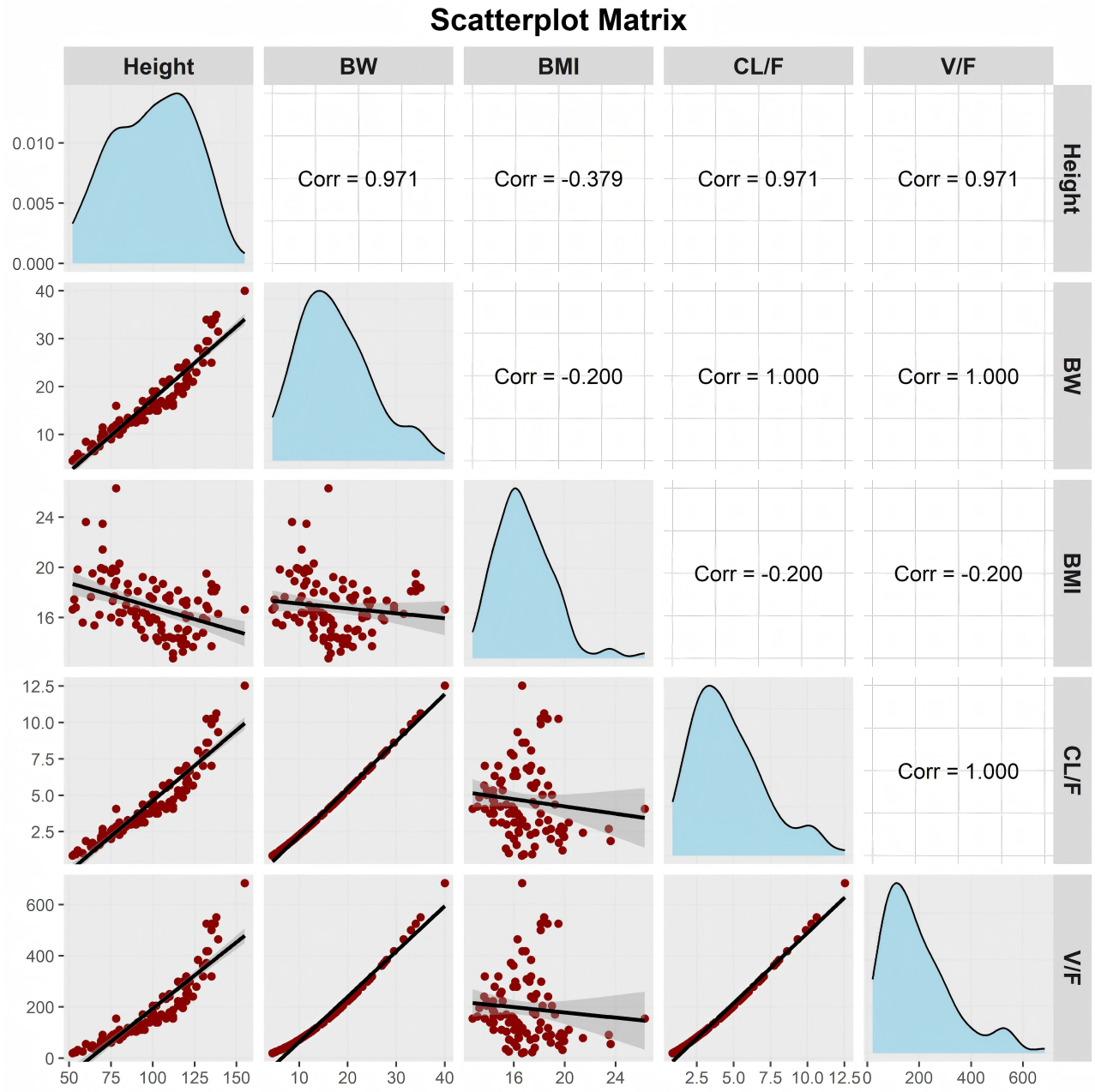

Figure 2 Scatterplot matrix of and pharmacokinetic parameters and related covariates.
Abbreviations: BW, body weight; BMI, body mass index; CL/F, apparent clearance; V/F, apparent distribution volume.

https://sirolimus-supra-therapeutic-risk-model.streamlit.app/). The interactive interfaces of these decision support tools are presented in Supplementary Figure S2.

Discussion

Given the clinical challenge of wide interindividual variability in drug exposure in vascular anomalies children, we developed six ML models based on multiple clinical characteristics to predict sub-therapeutic and supra-therapeutic sirolimus blood level risks. After comprehensive evaluation, we identified the MLP model as the optimal predictive model for subtherapeutic concentration risk and XGB model for supratherapeutic concentration risk, both demonstrating satisfactory predictive performance and clinical usability. To our knowledge, this is the first study to integrate ML

https://doi.org/10.2147/DDDT.S563637

Table 3 The Performance of ML Models of the Testing Set

Predict Outcome	Model	Cut-off	AUPRC	Accuracy	Precision	Recall	F1-score
Sub-therapeutic	LR	0.508	0.234	0.519	0.200	0.286	0.235
	XGB	0.299	0.286	0.556	0.333	0.714	0.455
	RFC	0.451	0.339	0.667	0.400	0.571	0.471
	SVM	0.286	0.288	0.333	0.211	0.571	0.308
	LGBM	0.512	0.414	0.593	0.300	0.429	0.353
	MLP	0.109	0.556	0.778	0.571	0.571	0.571
Supra-therapeutic	LR	0.496	0.295	0.556	0.286	0.667	0.400
	XGB	0.308	0.524	0.704	0.400	0.667	0.500
	RFC	0.451	0.353	0.741	0.444	0.667	0.533
	SVM	0.288	0.496	0.630	0.333	0.667	0.444
	LGBM	0.453	0.364	0.667	0.400	1.000	0.571
	MLP	0.277	0.540	0.556	0.286	0.667	0.400

Abbreviations: ML, machine learning; AUPRC, area under the precision–recall curve; LR, logistic regression; XGB, extreme gradient boosting; RFC, random forest classifier; SVM, support vector machine; LGBM, light gradient boosting machines; MLP, multilayer perceptron.

algorithms with multidimensional clinical features to provide dual risk prediction for both below- and above-target sirolimus concentrations.

Recently, there has been growing interest in applying ML algorithms to advance personalized medicine, enabling real-time drug monitoring and dose adjustments tailored based on individual patient characteristics. MLP is a particular type of neural network capable of modeling nonlinear relationships between features and suitable for datasets with complex structures or latent patterns.[48] XGB enhances predictive performance by iteratively constructing regression trees, wherein each split is selected to minimize error and subsequent trees are built to fit the residuals of the preceding ones.[49] In the current study, the MLP and XGB models as the best-performing model for sub-therapeutic and supra-therapeutic concentration risk prediction of sirolimus, respectively, which provided satisfactory discriminative ability and calibration (AUROC = 0.646, Brier = 0.190; AUROC = 0.825, Brier = 0.143, respectively). Meanwhile, we noted that the performances were comparable between the training and test sets, indicating no overfitting. More importantly, the data of the time-external verification cohort has demonstrated the usability of the models (AUROC = 0.678, Brier = 0.190; AUROC = 0.767, Brier = 0.178, respectively). In fact, the XGB method and deep neural networks are also the algorithms that have won the most times in the Kaggle competitions. The MLP and XGB ML models have been successfully implemented in the field of TDM, providing robust technical support for personalized treatment strategies.[35,42,50,51] Woillard et al developed XGB ML models to predict the exposure of mycophenolic acid and tacrolimus using a limited number of blood concentrations measurements, demonstrating superior performance compared to Bayesian estimation.[49,52] Adamiszak et al employed an MLP for the construction of artificial neural networks to optimize an HPLC-UV approach for the determination of fluconazole in human plasma and proved its clinical applicability.[53]

Notably, our study considered more than 28 features, including pharmacokinetic parameters such as CL/F and V/F, and ultimately selected the 10 most relevant ones to predict the risk of off-target concentrations. For the "black boxes" of ML models, SHAP algorithm was used to provide explanations of feature importance and prediction contributions post hoc in this study. SHAP mainly focuses on revealing the importance of each feature in the prediction, helping to identify factors that have a key impact on the prediction results.[54] The MLP model identified five predictive factors for sub-therapeutic sirolimus concentrations in descending order of importance: MCH, BMI, TBIL, WBC, and TG. While, the XGB model prioritized TC, height, and HDL, next PLT, last ALT levels for supra-therapeutic risk prediction.

In blood, sirolimus preferentially distribute into erythrocytes.[55] MCH is a key parameter of red blood cells. Higher MCH could be associated with an increased erythrocyte binding capacity for the drug, thereby reducing the fraction of free sirolimus available for hepatic metabolism and systemic clearance. A parallel mechanism has been suggested for tacrolimus, where binding to red blood cells is thought to limit metabolic accessibility and alter clearance.[56] Bilirubin, a breakdown product of hemoglobin from aging red blood cells, demonstrates various physiological effects such as

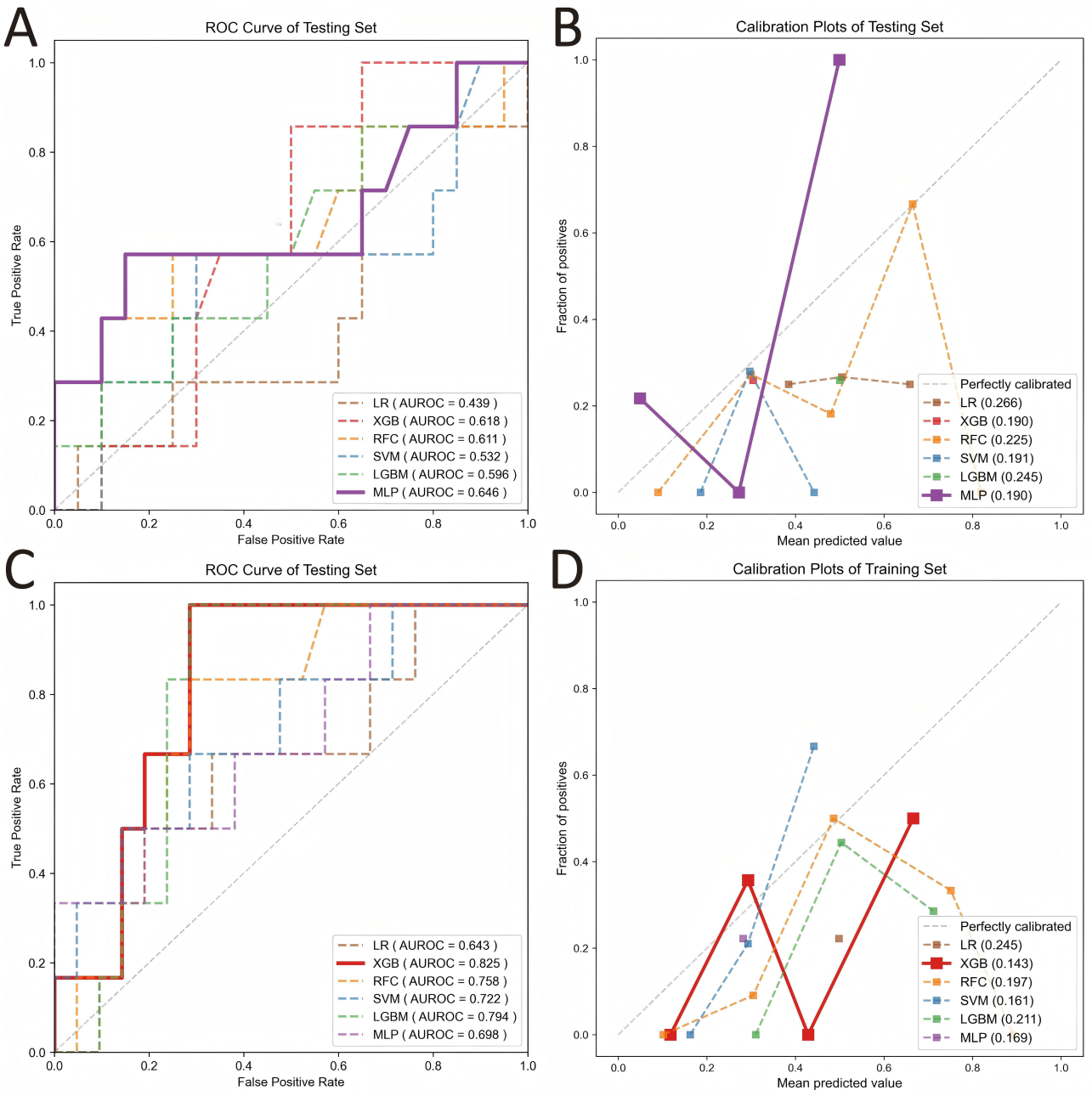

Figure 3 ROC and Calibration curves of six machine learning models on the testing set. (**A**) ROC curve and (**B**) Calibration curve of the " Sub-therapeutic" mo (**C**) ROC curve and (**D**) Calibration curve of the "Supra-therapeutic" model.

Abbreviations: AUROC, area under the receiver operating characteristic curve; LR, logistic regression, XGB, extreme gradient boosting, RFC, random forest classifier, SVM, support vector machine, LGBM, light gradient boosting machine, MLP, multilayer perceptron.

antioxidant, anti-inflammatory, and immunomodulatory functions.[57] Elevated TBIL levels may indicate underlying liver dysfunction,[58] which could compromise the activity of drug-metabolizing enzymes (eg, CYP3A4), leading to reduced clearance of sirolimus. This is supported by the observed negative association between TBIL and sirolimus CL/F.[59] Hence, higher TBIL levels may reduce sirolimus CL/F, theoretically increasing drug exposure.

As indicators of body size, height, BW, BSA, as well as BMI, are all regarded as significantly affecting sirolimus pharmacokinetics factors.[20] In fact, BW was the most commonly identified significant covariate in PopPK studies of sirolimus.[30–32,60–62] The influence of BW on V_d is commonly described using allometric scaling, a physiologically based approach grounded in the relationships between body size, blood volume, and vital capacity. However, on the present

https://doi.org/10.2147/DDDT.S563637

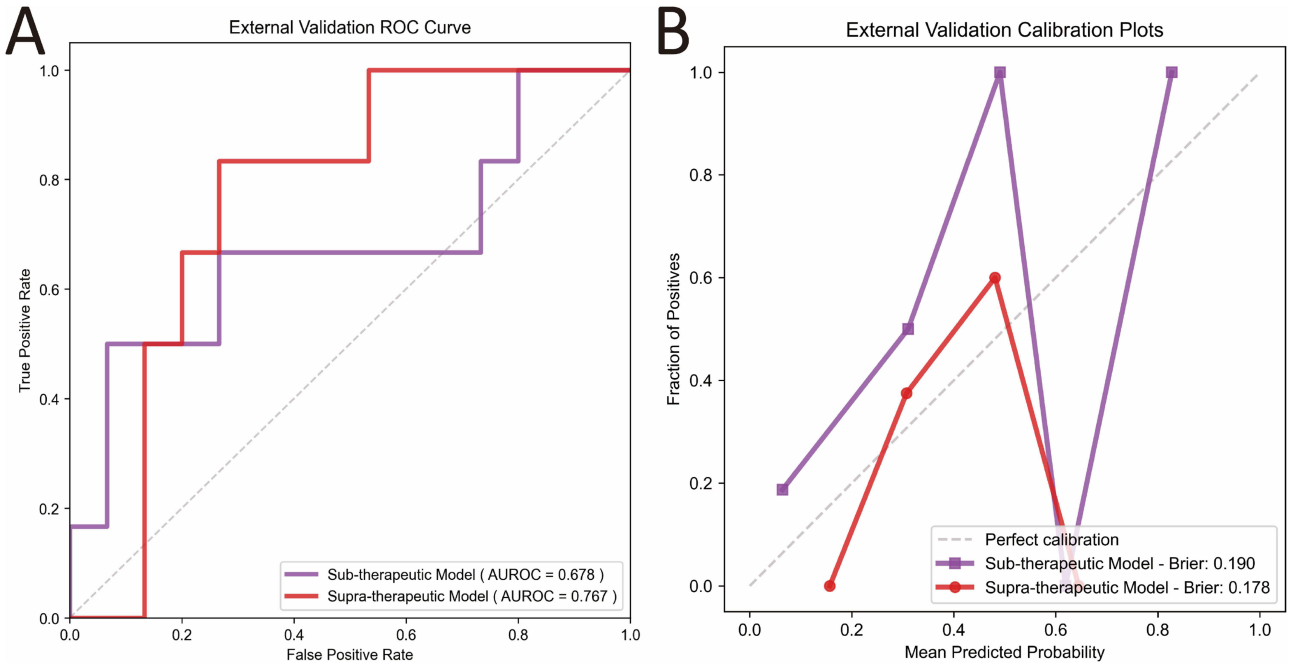

Figure 4 Performance evaluation of final models on temporal validation cohort. (**A**) ROC and (**B**) Calibration curves of sub-therapeutic model (MLP) and supra-therapeutic model (XGB).
Abbreviations: AUROC, area under the receiver operating characteristic curve; MLP, multilayer perceptron; XGB, extreme gradient boosting.

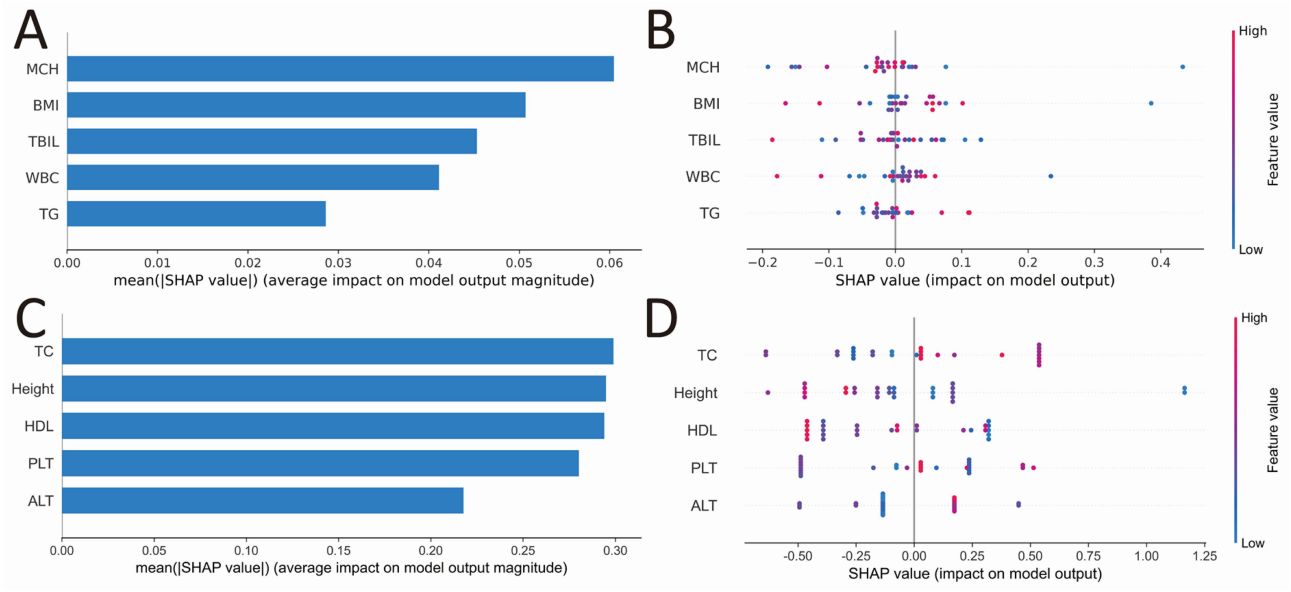

Figure 5 SHAP summary plots for the final predictive models. (**A**) Feature importance ranking and (**B**) beeswarm plot for individual features in the sub-therapeutic risk prediction model. (**C**) Feature importance ranking and (**D**) beeswarm plot for the supra-therapeutic risk prediction model.
Abbreviations: SHAP, SHapley Additive exPlanations; BMI, body mass index; WBC, white blood cell count; MCH, mean corpuscular hemoglobin; TG, triglycerides; TBIL, total bilirubin; PLT, platelet count; ALT, alanine aminotransferase; HDL, high-density lipoprotein cholesterol; TC, total cholesterol.

work, height was determined as a protective factor of supra-therapeutic concentration of sirolimus. This seems reasonable because of height exhibited a strong correlation with BW, CL/F and V/F in a matrix scatterplot analysis (Figure 2). In addition, height is an important variable during the period of development since our model covers children aged from 1 month to 12 years old.

https://doi.org/10.2147/DDDT.S563637

BMI is commonly used as a standardized measure for assessing population-level health risks, and is correlated with population adiposity levels. Adipose tissue, a metabolically active component constituting the major proportion of body weight, serves as a reservoir for lipophilic drugs, thereby altering their distribution and resulting in plasma concentration fluctuations. Moreover, obesity often alters the activity of drug-metabolizing enzymes and transporters, potentially affecting pharmacokinetic elimination.[63] For most investigated drugs, lipophilicity is a major determinant of the variability observed in peripheral volume of distribution estimates. For instance, the absolute V_d of a highly lipophilic drug, docetaxel, compare to obese patients, the volume of distribution at steady state increase is greater than 400 L in lean patients (V_{ss} = 531L vs 978L).[64] A previous study found that compared with the low-fat group, the C_0 and C_4 values of tacrolimus in the high-fat group were remarkably increased (P = 0.024 and 0.031, respectively).[65] Similar to tacrolimus, sirolimus is also a lipophilic drug,[66] the pharmacokinetics of this drug might be influenced by an individual's fat mass composition. Badri et al identified statistically significant differences in ideal body weight and adjusted body weight between patients with appropriate (5–15 ng/mL) and inappropriate sirolimus concentrations.[67] Consequently, BMI was identified as a risk factor in the sub-therapeutic concentration prediction model.

As is well known, hyperlipidemia was the typical adverse reaction of sirolimus.[68] Hyperlipidemia included the increase in TC and TG levels. Elevated TC levels are associated with an increased risk of supra-therapeutic sirolimus concentration. This finding is generally consistent with the earlier results reported by Jiao and colleagues,[61] who reported that lower sirolimus CL/F in patients with elevated TC. This may be due to elevated TC levels reducing the unbound drug fraction available for metabolism and elimination. Impaired metabolic and clearance of sirolimus is observed under dyslipidemia conditions. On the contrary, HDL-cholesterol commonly termed "good-cholesterol" because numerous epidemiological studies have shown that an inverse association between HDL cholesterol level and cardiovascular disease. HDL is critically involved in reverse cholesterol transport, the modulation of inflammation, the regulation of endothelial function, and the inhibition of low-density lipoprotein oxidation. It can help remove excess cholesterol from the body and reduce lipid burden.[69] Zahir et al reported that in heart transplant recipients, when serum TG exceeded 2 mmol/L, the apparent CL/F of sirolimus decreased by 37.8%.[70] Although TG was identified as a predictive factor for sub-therapeutic sirolimus concentrations in this study, its contribution to the MLP model is relatively weak. This seemingly contradictory observation result may be attributed to heterogeneity in patient populations and disease types, and the underlying mechanism requires further investigation.

Sirolimus is metabolized by CYP3A4 in liver.[71] Particularly, Livers from patients with severe chronic liver disease exhibited a 75% reduction in CYP3A concentration.[72] Previous studies demonstrated that in adult subjects with mild, moderate, and severe hepatic impairment, the whole-blood sirolimus weight-normalized oral clearance was reduced by 32%, 36%, and 67%, respectively, compared to healthy controls.[73,74] Serum ALT levels serve as a clinical indicator of hepatic function. Elevated ALT values often suggest hepatic impairment, which can reduce the hepatic clearance of sirolimus and lead to increased systemic exposure to the drug. This result is consistent with a TDM study by Xu and colleagues in pediatric patient, who recognized that ALT level serves as a key determinant affecting sirolimus blood concentrations.[75]

Furthermore, another key factor that has been mentioned to affect sirolimus concentration is PLT.[75] In our cohort, approximately 20% of the patients were diagnosed with KHE. The most common accompanying symptoms of KHE are thrombocytopenia and consumptive coagulopathy, which has a high risk of developing into Kasabach–Merritt phenomenon (KMP).[76] Ji et al reported that following sirolimus level stabilization at 10–15 ng/mL, all KMP patients demonstrated hematologic improvement, including PLT > 100×10^9/L.[77] Therefore, during KHE treatment, close monitoring of PLT is essential to prevent supra-therapeutic sirolimus concentrations and minimize adverse drug reaction risks.

The primary strength of the study lies in development of ML models that accurately and efficiently achieves bidirectional prediction of both sub-therapeutic and supra-therapeutic sirolimus concentrations in vascular anomalies pediatric patients. This innovative approach ensures maintained drug levels within the target therapeutic window of 10–15 ng/mL, providing clinicians with dual safeguards for effectively preventing both treatment failure and drug-induced toxicity. Additionally, sirolimus has a terminal elimination half-life of approximately 62 hours,[16] indicating that TDM should be conducted solely after reaching steady-state concentrations, a process requiring at least four half-lives after initiating or modifying therapy.[66] Our ML prediction models developed rely on clinically accessible data (height, BMI, routine laboratory test results), which collected during sirolimus administration or dose adjustment, serves as an early warning system. The risk prediction models

 https://doi.org/10.2147/DDDT.S563637

contribute to proactively identify individuals at heightened risk of exceeding the therapeutic window, enabling preemptive adjustments, which holds particular implications for cross-regional healthcare seekers and economically disadvantaged populations. Furthermore, we provided interactive web interfaces for sub-therapeutic and supra-therapeutic risk prediction models, significantly enhancing clinical utility through user-friendly application. Ultimately, the risk prediction model we constructed can reduce the need for frequent, invasive blood tests, enhanced the efficacy and safety of sirolimus therapy for children, supporting the implementation of personalized treatment plans.

There are several limitations in our study. Firstly, pharmacogenetic factors influencing sirolimus pharmacokinetics and pharmacodynamics of sirolimus were not incorporated into the predictive algorithms during model development. This decision was based on the following two considerations: (1) genetic data are not routinely available in standard clinical practice and (2) these pharmacogenetic variants were ultimately excluded from our previously established PPK model of sirolimus in vascular anomalies children,[30] consistent with findings from a dedicated pharmacogenetic study of sirolimus in low-flow vascular malformations.[17] Unlike the clinically significant influence of genetic variants observed in transplant recipients,[19,78,79] genetic polymorphisms appear to exert limited impact on sirolimus exposure in patients with vascular anomalies. If genetic testing becomes routine, reevaluation may be warranted for specific subpopulations of vascular anomalies. Secondly, although it is well established that cytochrome P450 (CYP) 3A inducers and inhibitors (eg, azole antifungals, cyclosporine A) significantly impact sirolimus exposure,[23,80,81] the limited number of patients receiving concomitant medications in this single-center retrospective study precluded meaningful evaluation of potential drug–drug interactions with sirolimus. Thirdly, the external validation dataset was derived from the same single institution, which may limit the generalizability of the model. Therefore, large-scale, multicenter studies are warranted to robustly evaluate the broader clinical applicability, reliability, and translational potential of our ML models.

Conclusion

To our knowledge, this is the first study to establish ML models using data from Chinese pediatric patients with vascular anomalies to predict the risk of sub-/supra-therapeutic sirolimus concentrations. The models can be selected based on available laboratory test results and actual needs, improving clinical utility. ML methods can effectively reduce the need for frequent concentration monitoring while maintaining optimal therapeutic levels, thereby enhancing treatment efficacy, minimizing adverse reactions, and facilitating the implementation of precision dosing strategies. However, additional validation studies and clinical refinements are required to ensure the robustness and generalizability of the models.

Data Sharing Statement

The data supporting the findings of this study are available from the corresponding author, Dr. Wei-Min Shen, upon reasonable request. Requests and proposals for data access should be directed to swmswmswm@sina.com and will be reviewed by the research team.

Ethics Statement

This retrospective study was approved by the Ethics Committee of Children's Hospital of Nanjing Medical University (Approval No.202206114-1). All data were de-identified prior to analysis to ensure patient confidentiality. The study was conducted in accordance with the principles of the Declaration of Helsinki and its later amendments.

Acknowledgments

This research was supported by the Research Project established by Chinese Pharmaceutical Association Hospital Pharmacy department (CPA-Z05-ZC-2023002), and the Hospital Pharmacy Foundation of Nanjing Pharmaceutical Association (2024YX003).

Author Contributions

All authors made a significant contribution to the work reported, whether that is in the conception, study design, execution, acquisition of data, analysis and interpretation, or in all these areas; took part in drafting, revising or critically

reviewing the article; gave final approval of the version to be published; have agreed on the journal to which the article has been submitted; and agree to be accountable for all aspects of the work.

Disclosure

The authors declare no conflicts of interest in this work.

References

1. Li J, Kim SG, Blenis J. Rapamycin: one drug, many effects. *Cell Metab*. 2014;19(3):373–379. doi:10.1016/j.cmet.2014.01.001
2. Roark KM, Iffland PH. Rapamycin for longevity: the pros, the cons, and future perspectives. *Front Aging*. 2025;6:1628187. doi:10.3389/fragi.2025.1628187
3. Queisser A, Seront E, Boon LM, et al. Genetic basis and therapies for vascular anomalies. *Circ Res*. 2021;129(1):155–173. doi:10.1161/CIRCRESAHA.121.318145
4. Zhou J, Lan Y, Qiu T, et al. Efficacy and safety of high-vs low-dose sirolimus in patients with kaposiform hemangioendothelioma: a randomized clinical trial. *J Am Acad Dermatol*. 2025;93(1):124–131. doi:10.1016/j.jaad.2025.03.023
5. ISSVA Classification of Vascular Anomalies ©2025 International Society for the Study of Vascular Anomalies. Available from: https://www.issva.org/classification. Accessed August 21, 2025.
6. Hammill AM, Wentzel M, Gupta A, et al. Sirolimus for the treatment of complicated vascular anomalies in children. *Pediatr Blood Cancer*. 2011;57(6):1018–1024. doi:10.1002/pbc.23124
7. Lackner H, Karastaneva A, Schwinger W, et al. Sirolimus for the treatment of children with various complicated vascular anomalies. *Eur J Pediatr*. 2015;174(12):1579–1584. doi:10.1007/s00431-015-2572-y
8. Nadal M, Giraudeau B, Tavernier E, et al. Efficacy and safety of mammalian target of rapamycin inhibitors in vascular anomalies: a systematic review. *Acta Derm Venereol*. 2016;96(4):448–452. doi:10.2340/00015555-2300
9. Adams DM, Trenor CC, Hammill AM, et al. Efficacy and safety of sirolimus in the treatment of complicated vascular anomalies. *Pediatrics*. 2016;137(2):e20153257. doi:10.1542/peds.2015-3257
10. Triana P, Dore M, Cerezo VN, et al. Sirolimus in the treatment of vascular anomalies. *Eur J Pediatr Surg*. 2017;27(1):86–90. doi:10.1055/s-0036-1593383
11. Hammer J, Seront E, Duez S, et al. Sirolimus is efficacious in treatment for extensive and/or complex slow-flow vascular malformations: a monocentric prospective Phase II study. *Orphanet J Rare Dis*. 2018;13(1):191. doi:10.1186/s13023-018-0934-z
12. Grenier PO, McCormack L, Alshamekh SA, et al. Mucocutaneous adverse events associated with oral sirolimus for the treatment of vascular anomalies. *JAMA Dermatol*. 2021;157(2):233–235. doi:10.1001/jamadermatol.2020.5180
13. McCormack FX, Inoue Y, Moss J, et al. Efficacy and safety of sirolimus in lymphangioleiomyomatosis. *N Engl J Med*. 2011;364(17):1595–1606. doi:10.1056/NEJMoa1100391
14. Seront E, Van Damme A, Legrand C, et al. Preliminary results of the European multicentric Phase III trial regarding sirolimus in slow-flow vascular malformations. *JCI Insight*. 2023;8(21). doi:10.1172/jci.insight.173095
15. Emoto C, Fukuda T, Cox S, et al. Development of a physiologically-based pharmacokinetic model for sirolimus: predicting bioavailability based on intestinal CYP3A content. *CPT Pharmacometrics Syst Pharmacol*. 2013;2(7):e59. doi:10.1038/psp.2013.33
16. Stenton SB, Partovi N, Ensom MH. Sirolimus: the evidence for clinical pharmacokinetic monitoring. *Clin Pharmacokinet*. 2005;44(8):769–786. doi:10.2165/00003088-200544080-00001
17. Wm Te Loo DM, Harbers V, Vermeltfoort L, et al. Influence of genetic variants on the pharmacokinetics and pharmacodynamics of sirolimus: a systematic review. *Pharmacogenomics*. 2023;24(11):629–639. doi:10.2217/pgs-2022-0147
18. Triana P, Miguel M, Díaz M, et al. Clinical monitoring challenges in the pharmacological treatment and management of lymphatic anomalies with mammalian target of rapamycin inhibition. *Ther Drug Monit*. 2019;41(4):547–548. doi:10.1097/FTD.0000000000000648
19. Shao S, Hu L, Han Z, et al. The effect of ABCB1 polymorphism on sirolimus in renal transplant recipients: a meta-analysis. *Transl Androl Urol*. 2020;9(2):673–683. doi:10.21037/tau.2020.03.42
20. Methaneethorn J, Art-Arsa P, Kosiyaporn R, et al. Predictors of sirolimus pharmacokinetic variability identified using a nonlinear mixed effects approach: a systematic review. *J Popul Ther Clin Pharmacol*. 2022;29(4):e11–e29. doi:10.47750/jptcp.2022.940
21. MacDonald A, Scarola J, Burke JT, et al. Clinical pharmacokinetics and therapeutic drug monitoring of sirolimus. *Clin Ther*. 2000;22(Suppl B):B101–121. doi:10.1016/S0149-2918(00)89027-X
22. Chueh SC, Wang S-M, Lai M-K, et al. Pharmacokinetic variability of sirolimus in Taiwanese renal transplant recipients. *Transplant Proc*. 2004;36(7):2058–2059. doi:10.1016/j.transproceed.2004.09.005
23. Cattaneo D, Merlini S, Pellegrino M, et al. Therapeutic drug monitoring of sirolimus: effect of concomitant immunosuppressive therapy and optimization of drug dosing. *Am J Transplant*. 2004;4(8):1345–1351. doi:10.1111/j.1600-6143.2004.00517.x
24. Ates HC, Alshanawani A, Hagel S, et al. Unraveling the impact of therapeutic drug monitoring via machine learning for patients with sepsis. *Cell Rep Med*. 2024;5(8):101681. doi:10.1016/j.xcrm.2024.101681
25. Freixo C, Ferreira V, Martins J, et al. Efficacy and safety of sirolimus in the treatment of vascular anomalies: a systematic review. *J Vasc Surg*. 2020;71(1):318–327. doi:10.1016/j.jvs.2019.06.217
26. Wiegand S, Wichmann G, Dietz A. Treatment of lymphatic malformations with the mtor inhibitor sirolimus: a systematic review. *Lymphat Res Biol*. 2018;16(4):330–339. doi:10.1089/lrb.2017.0062
27. Stillo F, Mattassi R, Diociaiuti A, et al. Guidelines for vascular anomalies by the Italian Society for the study of Vascular Anomalies (SISAV). *Int Angiol*. 2022;41(2 Suppl 1):1–130. doi:10.23736/S0392-9590.22.04902-1
28. Association, H.a.V.M.G.o.t.P.S.B.o.t.C.M. Diagnosis and treatment guideline for hemangiomas and vascular malformations (Chinese Medical Association 2024 version); 2024.

29. Mizuno T, Fukuda T, Emoto C, et al. Developmental pharmacokinetics of sirolimus: implications for precision dosing in neonates and infants with complicated vascular anomalies. *Pediatr Blood Cancer*. 2017;64(8). doi:10.1002/pbc.26470
30. Fan L, Guo H-L, Zhao Y-T, et al. Population pharmacokinetic study in children with vascular anomalies: body weight as a key variable in predicting the initial dose and dosing frequency of sirolimus. *Front Pharmacol*. 2024;15:1457614. doi:10.3389/fphar.2024.1457614
31. Liu B, Zhang X, Zhao Y, et al. Model-Informed individualized dosage regimen of sirolimus in pediatric patients with intractable lymphatic malformations. *Eur J Pharm Sci*. 2024;200:106837. doi:10.1016/j.ejps.2024.106837
32. Chen X, Wang -D-D, Xu H, et al. Initial dose recommendation for sirolimus in paediatric kaposiform haemangioendothelioma patients based on population pharmacokinetics and pharmacogenomics. *J Int Med Res*. 2020;48(8):300060520947627. doi:10.1177/0300060520947627
33. Hu YH, Zhao Y-T, Guo H-L, et al. Therapeutic drug monitoring for sirolimus in children with vascular anomalies: what can we learn from a retrospective study. *Pharmaceuticals*. 2024;17(10):1255. doi:10.3390/ph17101255
34. Chen K, Wang C, Wei Y, et al. Machine learning and population pharmacokinetics: a hybrid approach for optimizing vancomycin therapy in sepsis patients. *Microbiol Spectr*. 2025;13(5):e0049925. doi:10.1128/spectrum.00499-25
35. Curth A, Peck RW, McKinney E, et al. Using machine learning to individualize treatment effect estimation: challenges and opportunities. *Clin Pharmacol Ther*. 2024;115(4):710–719. doi:10.1002/cpt.3159
36. Poweleit EA, Vinks AA, Mizuno T. Artificial intelligence and machine learning approaches to facilitate therapeutic drug management and model-informed precision dosing. *Ther Drug Monit*. 2023;45(2):143–150. doi:10.1097/FTD.0000000000001078
37. Bram DS, Parrott N, Hutchinson L, et al. Introduction of an artificial neural network-based method for concentration-time predictions. *CPT Pharmacometrics Syst Pharmacol*. 2022;11(6):745–754. doi:10.1002/psp4.12786
38. Grossen AA, Evans AR, Ernst GL, et al. The current landscape of machine learning-based radiomics in arteriovenous malformations: a systematic review and radiomics quality score assessment. *Front Neurol*. 2024;15:1398876. doi:10.3389/fneur.2024.1398876
39. Zhu H, Liu L, Liang S, et al. Rupture risk assessment in cerebral arteriovenous malformations: an ensemble model using hemodynamic and morphological features. *J Neurointerv Surg*. 2025;17:1089–1095. doi:10.1136/jnis-2024-022208
40. Jiao B, Wang L, Zhang X, et al. MRI-based radiomics model for the preoperative prediction of classification in children with venous malformations. *Clin Radiol*. 2025;87:106966. doi:10.1016/j.crad.2025.106966
41. Zhao J, Dai S, He J, et al. Prediction of high-dose methotrexate blood concentration in osteosarcoma patients using machine learning. *Drug Des Devel Ther*. 2025;19:3631–3643. doi:10.2147/DDDT.S515535
42. Guo W, Yu Z, Gao Y, et al. A machine learning model to predict risperidone active moiety concentration based on initial therapeutic drug monitoring. *Front Psychiatry*. 2021;12:711868. doi:10.3389/fpsyt.2021.711868
43. Zhao YT, Dai H-R, Li Y, et al. Comparison of LC-MS/MS and EMIT methods for the precise determination of blood sirolimus in children with vascular anomalies. *Front Pharmacol*. 2022;13:925018. doi:10.3389/fphar.2022.925018
44. Zheng P, Yu Z, Li L, et al. Predicting blood concentration of tacrolimus in patients with autoimmune diseases using machine learning techniques based on real-world evidence. *Front Pharmacol*. 2021;12:727245. doi:10.3389/fphar.2021.727245
45. Ji Y, Chen S, Yang K, et al. A prospective multicenter study of sirolimus for complicated vascular anomalies. *J Vasc Surg*. 2021;74(5):1673–1681e3. doi:10.1016/j.jvs.2021.04.071
46. Vasquez MM, Hu C, Roe DJ, et al. Least absolute shrinkage and selection operator type methods for the identification of serum biomarkers of overweight and obesity: simulation and application. *BMC Med Res Methodol*. 2016;16(1):154. doi:10.1186/s12874-016-0254-8
47. Fluss R, Faraggi D, Reiser B. Estimation of the Youden Index and its associated cutoff point. *Biom J*. 2005;47(4):458–472. doi:10.1002/bimj.200410135
48. Luo Y, Ding W, Yang X, et al. Construction and validation of a predictive model for meningoencephalitis in pediatric scrub typhus based on machine learning algorithms. *Emerg Microbes Infect*. 2025;14(1):2469651. doi:10.1080/22221751.2025.2469651
49. Woillard JB, Labriffe M, Debord J, et al. Tacrolimus exposure prediction using machine learning. *Clin Pharmacol Ther*. 2021;110(2):361–369. doi:10.1002/cpt.2123
50. Woillard JB, Labriffe M, Marquet P. Estimation of overall cyclosporine exposure using machine learning. *Ther Drug Monit*. 2025;47:779–789. doi:10.1097/FTD.0000000000001346
51. Huang X, Yu Z, Bu S, et al. An ensemble model for prediction of vancomycin trough concentrations in pediatric patients. *Drug Des Devel Ther*. 2021;15:1549–1559. doi:10.2147/DDDT.S299037
52. Woillard JB, Labriffe M, Debord J, et al. Mycophenolic acid exposure prediction using machine learning. *Clin Pharmacol Ther*. 2021;110(2):370–379. doi:10.1002/cpt.2216
53. Adamiszak A, Czyrski A, Sznek B, et al. The application of the design of experiments and artificial neural networks in the development of a fast and straightforward HPLC-UV method for fluconazole determination in hemato-oncologic pediatric patients and its adaptation to therapeutic drug monitoring. *Pharmaceuticals*. 2024;17(12).
54. Huang S, Xu Q, Yang G, et al. Machine learning for prediction of drug concentrations: application and challenges. *Clin Pharmacol Ther*. 2025;117(5):1236–1247. doi:10.1002/cpt.3577
55. Yatscoff R, LeGatt D, Keenan R, et al. Blood distribution of rapamycin. *Transplantation*. 1993;56(5):1202–1206. doi:10.1097/00007890-199311000-00029
56. Zheng S, Easterling TR, Umans JG, et al. Pharmacokinetics of tacrolimus during pregnancy. *Ther Drug Monit*. 2012;34(6):660–670. doi:10.1097/FTD.0b013e3182708edf
57. Zhang Y, Luan H, Song P. Bilirubin metabolism and its application in disease prevention: mechanisms and research advances. *Inflamm Res*. 2025;74(1):81. doi:10.1007/s00011-025-02049-w
58. Kipp ZA, Pauss SN, Martinez GJ, et al. Bilirubin hepatic and intestinal transport and catabolism: physiology, pathophysiology, and benefits. *Antioxidants*. 2025;14(11):1326. doi:10.3390/antiox14111326
59. Cheng X, Zhao Y, Gu H, et al. The first study in pediatric: population pharmacokinetics of sirolimus and its application in Chinese children with immune cytopenia. *Int J Immunopathol Pharmacol*. 2020;34:2058738420934936. doi:10.1177/2058738420934936
60. Sato E, Shimomura M, Masuda S, et al. Temporal decline in sirolimus elimination immediately after pancreatic islet transplantation. *Drug Metab Pharmacokinet*. 2006;21(6):492–500. doi:10.2133/dmpk.21.492
61. Jiao Z, Shi X-J, Li Z-D, et al. Population pharmacokinetics of sirolimus in de novo Chinese adult renal transplant patients. *Br J Clin Pharmacol*. 2009;68(1):47–60. doi:10.1111/j.1365-2125.2009.03392.x

62. Mizuno T, Emoto C, Fukuda T, et al. Model-based precision dosing of sirolimus in pediatric patients with vascular anomalies. *Eur J Pharm Sci*. 2017;109S:S124–S131. doi:10.1016/j.ejps.2017.05.037
63. Hanley MJ, Abernethy DR, Greenblatt DJ. Effect of obesity on the pharmacokinetics of drugs in humans. *Clin Pharmacokinet*. 2010;49(2):71–87. doi:10.2165/11318100-000000000-00000
64. Sparreboom A, Wolff AC, Mathijssen RHJ, et al. Evaluation of alternate size descriptors for dose calculation of anticancer drugs in the obese. *J Clin Oncol*. 2007;25(30):4707–4713. doi:10.1200/JCO.2007.11.2938
65. Han SS, Kim DH, Lee SM, et al. Pharmacokinetics of tacrolimus according to body composition in recipients of kidney transplants. *Kidney Res Clin Pract*. 2012;31(3):157–162. doi:10.1016/j.krcp.2012.06.007
66. Mahalati K, Kahan BD. Clinical pharmacokinetics of sirolimus. *Clin Pharmacokinet*. 2001;40(8):573–585. doi:10.2165/00003088-200140080-00002
67. Badri S, Dadkhah-Tehrani B, Atapour A, et al. The relationship between weight indices and blood levels of immunosuppressive drugs in renal transplant recipients. *Iran J Pharm Res*. 2024;23(1):e146619. doi:10.5812/ijpr-146619
68. Wiegand S, Dietz A, Wichmann G. Efficacy of sirolimus in children with lymphatic malformations of the head and neck. *Eur Arch Otorhinolaryngol*. 2022;279(8):3801–3810. doi:10.1007/s00405-022-07378-8
69. Playford MP, Neufeld EB, Zubirán R, et al. Reverse cholesterol transport: current assay methods, alterations with disease and response to therapeutic intervention. *Front Cardiovasc Med*. 2025;12:1608384. doi:10.3389/fcvm.2025.1608384
70. Zahir H, Keogh A, Akhlaghi F. Apparent clearance of sirolimus in heart transplant recipients: impact of primary diagnosis and serum lipids. *Ther Drug Monit*. 2006;28(6):818–826. doi:10.1097/01.ftd.0000246765.05248.fa
71. Shen G, Moua KTY, Perkins K, et al. Precision sirolimus dosing in children: the potential for model-informed dosing and novel drug monitoring. *Front Pharmacol*. 2023;14:1126981. doi:10.3389/fphar.2023.1126981
72. George J, Murray M, Byth K, et al. Differential alterations of cytochrome P450 proteins in livers from patients with severe chronic liver disease. *Hepatology*. 1995;21(1):120–128.
73. Zimmerman JJ, Lasseter KC, Lim H-K, et al. Pharmacokinetics of sirolimus (rapamycin) in subjects with mild to moderate hepatic impairment. *J Clin Pharmacol*. 2005;45(12):1368–1372. doi:10.1177/0091270005281350
74. Zimmerman JJ, Patat A, Parks V, et al. Pharmacokinetics of sirolimus (rapamycin) in subjects with severe hepatic impairment. *J Clin Pharmacol*. 2008;48(3):285–292. doi:10.1177/0091270007312902
75. Xu X, Mao X, Liu B, et al. Analysis of sirolimus blood concentration and influencing factors in pediatric patients: implications for individualized drug therapy. *Drugs R D*. 2025;25(1):79–88. doi:10.1007/s40268-025-00506-9
76. Li M, Wang X, Kieran R, et al. Treatment experience for different risk groups of Kaposiform hemangioendothelioma. *Front Oncol*. 2024;14:1336763. doi:10.3389/fonc.2024.1336763
77. Ji Y, Chen S, Xiang B, et al. Sirolimus for the treatment of progressive kaposiform hemangioendothelioma: a multicenter retrospective study. *Int J Cancer*. 2017;141(4):848–855. doi:10.1002/ijc.30775
78. Park YA, Park J, Yee J, et al. Effects of CYP3A5 genetic polymorphisms on the weight-adjusted through concentration of sirolimus in renal transplant recipients: a systematic review and meta-analysis. *Curr Pharm Des*. 2024;30(39):3108–3115. doi:10.2174/0113816128324199240730093415
79. Liu J, Feng D, Kan X, et al. Polymorphisms in the CYP3A5 gene significantly affect the pharmacokinetics of sirolimus after kidney transplantation. *Pharmacogenomics*. 2021;22(14):903–912. doi:10.2217/pgs-2021-0083
80. Scherkl C, Meid AD, Cuntz SE, et al. Coadministration of fluconazole to boost subtherapeutic sirolimus concentrations: a case report. *Pharmacol Res Perspect*. 2024;12(3):e1198. doi:10.1002/prp2.1198
81. Boni JP, Leister C, Burns J, et al. Differential effects of ketoconazole on exposure to temsirolimus following intravenous infusion of temsirolimus. *Br J Cancer*. 2008;98(11):1797–1802. doi:10.1038/sj.bjc.6604376